A Comparison of a Mean Field Theoretic Approach to Ferromagnetism with Experimental Results in $Nd_2Fe_{14}B$ Magnets

Patrick Yarbrough
Department of Physics and Engineering, Fort Lewis College, Colorado, United States

Often, trying to describe how atomic interactions in a structure come to manifest themselves macroscopically is tedious if not impossible when large numbers of molecules or atoms are being considered. One way to more easily approximate the expected behavior of a large system of particles, such as magnetic dipoles, is to consider how the "mean field" produced by neighboring particles near a single particle affects it. In magnetic systems, there is an electromagnetic exchange between individual dipoles that extends only negligibly beyond the other dipoles immediately adjacent to them. By "tagging" an individual dipole in a tetragonal crystal lattice of ferromagnetic dipoles and then "freezing" the dipoles immediately near it, the mean field produced by the frozen dipoles can be calculated, and the net effect of the mean field on the tagged dipole can be seen. In the case of ferromagnetism (and all magnetic systems), the magnetization and orientations of dipoles are dependent on temperature. To see this, $Nd_2Fe_{14}B$ magnets were cooled with liquid nitrogen and allowed to warm back up to room temperature while the strength of their magnetic fields were measured at a constant distance. The observed field strengths are then compared with theoretical results produced from the mean field approximation.

I. Mean Field Theories

The behaviors of many- bodied systems of interacting particles are difficult to model as the number of particles being considered increases. For example, the interactions of two or three magnetic dipoles are easy enough to model directly, but trying to model real- world magnets with many orders of magnitude of particles becomes arduous. To resolve this problem, a mean field theoretic approach is taken to consider only the interactions of a single dipole with the dipoles immediately surrounding it, and generalizing this to the system as a whole[i].

The simplest of mean field theories are one- dimensional, such as the one-dimensional Ising model, in which a "string" of dipoles are considered; with one dipole being tagged and looking at the way the dipoles on either side of it affect its behavior. As the dimensionality of the system being considered increases, higher fidelity is reached to predict the behavior of the dipole being observed.

One application of mean field theory is to predict the temperature dependence of the magnetization in a ferromagnet. As ferromagnets are cooled their magnetic dipoles collapse into an aligned state that is energetically favorable, thus increasing the overall magnetization and field strength of the magnet. As a corollary to this, there exists a critical, or Curie, temperature above which a magnet loses all spontaneous magnetization and ceases to have a net magnetic moment. By taking into account the thermal energy and magnetic interactions of a system, the magnetic behavior of the system can be found. By treating individual crystals within the magnet as individual dipoles, a superposition principle is used to predict the behavior of the magnet as a whole when the total number of dipoles is known.

II. Theoretical considerations

The average spin alignment of a single dipole in a magnetic field is calculated as

$$\langle s_i \rangle = \tanh\left(\frac{\mu H}{kT}\right) \quad (1)$$

For a real magnetic system, such as a $Nd_2Fe_{14}B$ magnet, the interactions a single dipole has with the six dipoles surrounding it are considered. In this case, a single tetragonal crystal, rather than individual atoms within the crystalline structure, will be considered a single dipole. If the material is immersed in an external magnetic field, the energy of the system is given by

$$E = -\frac{J}{\mu}\sum_j s_j \, \mu \, s_i \; - \mu H \sum_i s_i \quad (2)$$

where J is a coupling constant used to describe the exchange interaction between two dipoles, s_i is the tagged dipole being observed, s_j are the surrounding dipoles, μ is the magnetic dipole moment and H is the applied external field. Since individual crystals, rather than individual atoms, are being treated as single dipoles, the exchange interaction and magnetic dipole moment is the same for all dipoles.

Equation (2) can be rewritten as

$$E = -\left(\frac{J}{\mu}\sum_j s_j\right)\mu s_i - \; H\mu s_i \quad (3)$$

which suggests that the term in parenthesis has the form of a magnetic field given by

$$\left(\frac{J}{\mu}\sum_j s_j\right) = H_{eff}$$

which implies

$$H_{eff} = \frac{J}{\mu}\sum_j s_j = \frac{nJ}{\mu}\langle s \rangle \quad (4)$$

The effective field of the surrounding dipoles on the tagged dipole is given by the average magnetization of the n nearest neighbors. To make an approximation for a ferromagnet, the external field is set equal to zero, and the magnetic field in (1) is given by H_{eff} to get

$$\langle s \rangle = \tanh\left(\frac{nJ\langle s \rangle}{kT}\right) \quad (5)$$

The subscript in (1) has been dropped since, after the system has come to equilibrium, the average spin of the tagged dipole will take on the same value as the average spin of the neighboring dipoles[ii].

The magnetization of a system is defined as $M = n\mu\langle s \rangle$ and the saturation magnetization is defined as $M_s = n\mu$, since at saturation, all dipoles in the system will have $\langle s \rangle = 1$. By noting that the average spin alignment is given by the ratio of the magnetization of the system to its saturation magnetization, and that the Curie temperature can be defined as

$$T_c = \frac{nJ}{k} \quad (6)$$

Equation (5) becomes

$$\frac{M}{M_s} = \tanh\left(\frac{T_c}{T}\frac{M}{M_s}\right) \quad (7)$$

Equation (7) is transcendental and can be solved graphically by plotting the left side ande right sides as functions of M/M_s , and finding where they intersect. When the ratio $T_c/T = 1$, there is only one solution to (7) at $M/M_s = 0$ suggesting that once the temperature of the system is greater than or equal to the Curie temperature, the thermal energy of the system overwhelms the magnetic interactions between dipoles, so the spontaneous magnetization in the system becomes zero. Once the temperature drops below the Curie temperature, magnetic interactions between dipoles cause spontaneous magnetization in the system to occur. Below the Curie temperature, there are three solutions to (7): one at $M/M_s = 0$, and two others that are equal and opposite to each other (since the system has no preference toward being spin up or spin down), which indicate the spontaneous magnetization of the system at a given temperature. Sample solutions to (7) are given in figure 1.

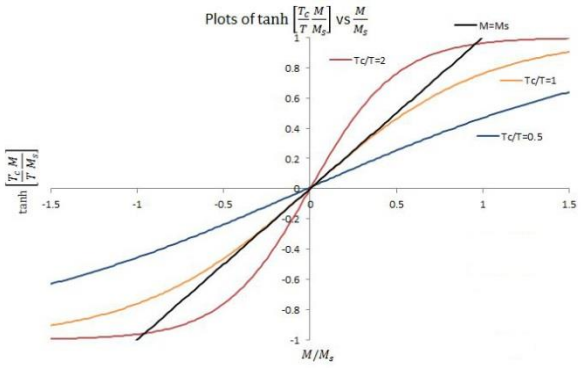

Figure 1 Solutions to (7) given by intersections the linear curve of the left side of (7) has with the hyperbolic tangent on the right side of (7). For temperatures below the Curie temperature, there are three solutions to (7), which indicate that spontaneous magnetization has occurred within the system.

However, (7) can be manipulated by recalling the definition of the hyperbolic tangent to get equation (8)[iii]

$$\frac{T}{T_c} = \frac{2M}{M_s} \Big/ \left(ln\left(1+\frac{M}{M_s}\right) - ln\left(1-\frac{M}{M_s}\right)\right) \quad (8)$$

With equation (8) theoretical predictions for the magnetization of the system as a function of temperature can be made.

III. Theoretical Predictions

Neodymium rare earth magnets, which have the composition $Nd_2Fe_{14}B$, form tetragonal crystals in which the Nd atoms have uniaxial or easy axis anisotropy. Equation (8) is used to predict the behavior of a ferromagnetic system, as shown in figure 2.

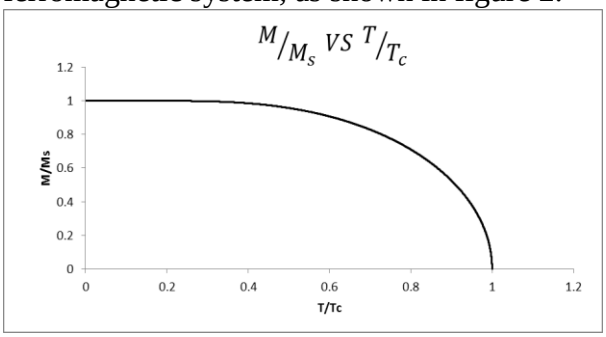

Figure 2 The normalized magnetization of a system is plotted as a function of the normalized temperature. Clearly as the normalized temperature reaches unity, the normalized spontaneous magnetization of the system goes to zero.

The Curie temperature for this type of magnet is well documented as 583K, and, by finding the magnetic dipole moment of a single crystal multiplied by the number of crystals in the magnet, the saturation magnetization of the system tested is found, enabling real values to be calculated[iv]. Using the predicted magnetizations of the magnet at various temperatures, the expected magnetic field intensity can be calculated by first considering the relation

$$\mathbf{H} = -\nabla\Psi$$

where Ψ is the scalar magnetic potential. Using the flux continuity law and knowing that Ψ must satisfy Poisson's equation, we find that

$$\Psi = \int_{S'} \frac{\sigma_m(\boldsymbol{r}')\rho' d\rho'}{4\pi\mu_o|\boldsymbol{r}-\boldsymbol{r}'|}$$

The magnetization of the magnet can be treated as being generated by surface bound currents, and so Ψ is calculated as a surface integral based on the geometry of each magnet[v]. If the magnetic field of a magnet is measured directly above the axis of magnetization, only the z component of the magnetic field intensity needs to be calculated.

For a disc shaped magnet, as depicted in figure 3, the z component of the magnetic field intensity is calculated as

$$\boldsymbol{H_z} = -\frac{dM}{2}\left[\frac{\left(\frac{z}{d}-\frac{1}{2}\right)}{\sqrt{\frac{R^2}{d}+\left(\frac{z}{d}-\frac{1}{2}\right)^2}} - \frac{\left(\frac{z}{d}+\frac{1}{2}\right)}{\sqrt{\frac{R^2}{d}+\left(\frac{z}{d}+\frac{1}{2}\right)^2}}\right] \quad (9)$$

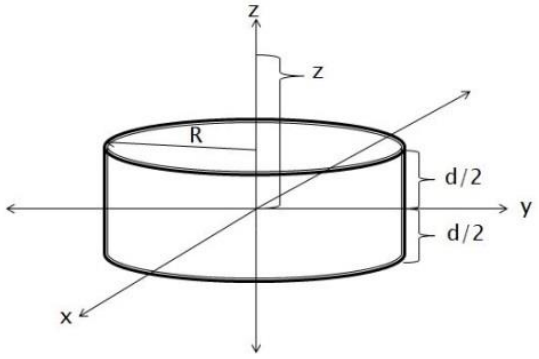

Figure 3 The geometry of a $Nd_2Fe_{14}B$ magnet tested. Equation (9) is based on the geometric configuration of the system to be tested.

By finding the magnetization of the system calculated in equation (8) and plugging these values into equation (9), theoretical predictions for the magnetic field of the disc shaped magnet in figure 2 as a function of temperature can be made. After converting magnetic field strength to magnetic flux density, theoretical predictions for the magnetic flux density of the $Nd_2Fe_{14}B$ magnet at a distance of z = 9.3 cm are given by figure 4.

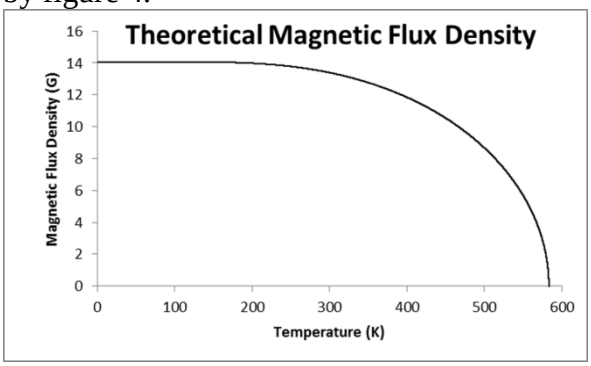

Figure 4 The theoretical magnetic flux density for a disc shaped magnet of radius 12.7 mm and height 9.53 mm a distance 9.3 cm above the magnet.

IV. Experimental Results

To observe the temperature dependence of the magnetic flux density described in figure 3, a T-type thermocouple is attached to the top of the magnet, while the magnet is placed in a Styrofoam vessel that is then filled with liquid nitrogen. Once the magnet is cooled to 77K and the liquid nitrogen has boiled away, voltages induced in a Hall Effect probe by the magnetic field are recorded as the magnet slowly rises to room temperature.

To make calculations simpler, the Hall Effect probe is placed directly above the magnet and voltages are measured to observe the radial strength of the magnetic field.

A typical example of the magnetic field strength compared with theoretical predictions in a $Nd_2Fe_{14}B$ magnet is shown in figure 5.

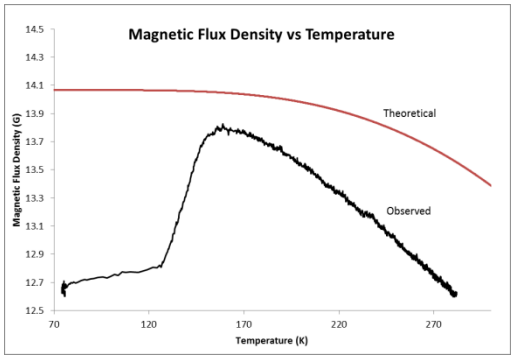

Figure 5 The observed magnetic flux density in the disc shaped magnet compared with the theoretical curve over the temperature range from 77K to 281.9K.

The observed magnetic flux density follows a trend similar to the theoretical predictions from 158.8K to 281.9K, when data recording stopped. Below 158.8K, the observed field strength in the magnet sharply declines, before starting to level out at 126.4K. This is due to a spin reorientation transition in which the material changes from having a uniaxial anisotropy to an easy-cone anisotropy[vi].

Ultimately, mean field theory is unreliable for materials that experience a spin reorientation transition (SRT). However, at temperatures above the SRT, the data may still be compared with theoretical predictions for $Nd_2Fe_{14}B$. A Taylor polynomial is fitted to the observed data over the temperature range from 158.8K to 281.9K and compared to theoretical predictions. There is found to be a 4.12% error in measurement of data, and the Taylor polynomial is plotted with error bars in figure 6.

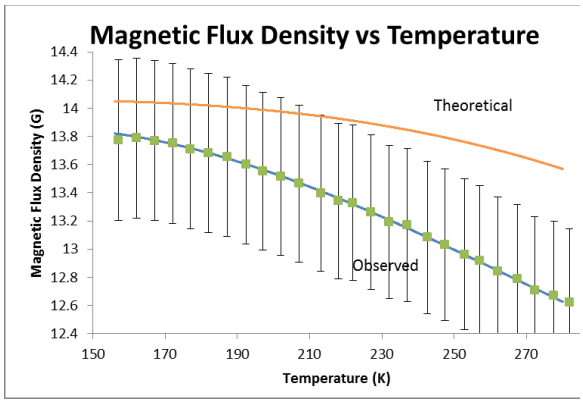

Figure 6 The observed magnetic flux density at temperatures above the SRT temperature with error bars compared with the theoretical curve.

At low temperatures from 158.8K up to about 219.5K, the theoretical curve lies within the region of error of observed data. This suggests that the mean field approximation produced reasonable results at low temperatures, although the discrepancy between the observed and theoretical curves gets larger as the temperature increases toward 281.9K. Over the entire temperature range being analyzed, mean field theory predicted values an average of 4.35% higher than the observed magnetic field.

V. Conclusions

At temperatures below room temperature, the Mean Field Theory provided relatively accurate predictions for the magnetic flux density in the magnets being tested. However, once the temperature dropped below 158.8K, a spin reorientation transition took place within the material which caused the observed magnetic field to decrease rapidly. Therefore, since the mean field theory makes no account of this transition, it is unreliable as a model for the behavior of the $Nd_2Fe_{14}B$ magnet below 158.8K. However, for other magnetic materials such as $Fe(III)O_2$ that do not experience this phenomena, the mean field theory may provide more accurate results.

The spin reorientation transition is not thought to decrease the magnetic field by more than 14%, gradually decreasing as the temperature drops toward 0K. Taking this into account along with the mean field theory, qualitative predictions for the behavior of a $Nd_2Fe_{14}B$ magnet can be made for cryogenic temperatures.

Acknowledgments

The funding to make this research possible was provided by an undergraduate research grant from the School of Natural and Behavioral Sciences at Fort Lewis College. The author would furthermore like to thank Drs. Jerry Crawford, Ryan Haaland and Randy Palmer for their oversight and input.

Appendix I- Theoretical Derivations

Exercise 1: A single dipole in an external magnetic field

Let the dipole be denoted by s_i , the magnetic dipole moment of s_i by μ, and the external magnetic field by H_{ext}. The dipole has two possible states: spin up (aligned with H_{ext}) or spin down (antiparallel to H_{ext}). These definitions are arbitrary and could be switched.
The energy of the dipole is given by

$$E = -\boldsymbol{\mu} \cdot \boldsymbol{H_{ext}} \quad (1)$$

Spin up: $$E_+ = -\mu H_{ext} \quad (2)$$

Spin down: $$E_- = +\mu H_{ext} \quad (3)$$

where spin up is the lower energy state, since it is energetically favorable for the dipole to be aligned with the external field. Similarly, the spin down state is the higher energy state, since it is energetically unfavorable for the dipole to be aligned opposite of the external field.
The probabilities of the dipole being spin up or spin down can be calculated with Boltzmann factors

Probability of spin up $$P_{-} = \frac{1}{\mathcal{Z}} e^{-\frac{\mu H_{ext}}{kT}} \quad (4)$$

Probability of spin down $$P_{+} = \frac{1}{\mathcal{Z}} e^{+\frac{\mu H_{ext}}{kT}} \quad (5)$$

Partition Function $$\mathcal{Z} = \sum_{E(s)} e^{-\frac{E(s)}{kT}} = e^{\frac{\mu H_{ext}}{kT}} + e^{-\frac{\mu H_{ext}}{kT}} \quad (6)$$

where k is Boltzmann's constant, and T is the absolute temperature of the system. The average thermal state of our dipole, denoted by $\langle s_i \rangle$, can be found by summing the probabilities of states multiplied by each state.

$$\langle s_i \rangle = \sum_{s_i = \pm 1} s_i P_{\pm} = (+1)P_{+} + (-1)P_{-} = \frac{e^{\frac{\mu H}{kT}}}{\mathcal{Z}} - \frac{e^{-\frac{\mu H}{kT}}}{\mathcal{Z}} \quad (7)$$

$$\langle s_i \rangle = \frac{e^{\frac{\mu H}{kT}} - e^{-\frac{\mu H}{kT}}}{e^{\frac{\mu H}{kT}} + e^{-\frac{\mu H}{kT}}} = \frac{sinh\ \frac{\mu H}{kT}}{cosh \frac{\mu H}{kT}} = tanh\left(\frac{\mu H}{kT}\right) \quad (8)$$

Exercise 2: a 2D lattice of dipoles in an external magnetic field

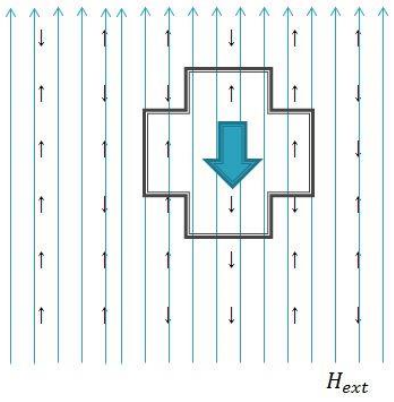

Consider the 2 dimensional lattice of dipoles as shown, in an external magnetic field. Let the dipole in the center be denoted by s_i and let the surrounding dipoles be denoted by the index s_j
The energy of the system is given by

$$E = -\frac{J}{\mu} \sum_{j} s_j \ \mu s_i - H_{ext} \mu s_i \quad (9)$$

where the first term on the right side of (9) is the sum of the interactions between s_i and each s_j dipole, and J is the average exchange interaction between the dipoles. The second term on the right side of (9) is the energy of s_i due to its interaction with the external magnetic field. If we take

$$-\frac{J}{\mu}\sum_j s_j\ \mu\ s_i\ = -\left(\frac{J}{\mu}\sum_j s_j\ \right)\frac{s_i}{\mu} \tag{10}$$

We can note that the term in parenthesis can be written as an effective magnetic field felt by s_i due to the s_j dipoles surrounding it.

$$\left(\frac{J}{\mu}\sum_j s_j\ \right) = H_{eff} \tag{11}$$

Since every s_j is the same, we can drop the subscript and take their average multiplied by the number of them, n.

$\langle s\rangle = \frac{1}{n}\sum_j s_j$ then

$$H_{eff} = \frac{J}{\mu}(n\langle s\rangle) = \frac{nJ}{\mu}\langle s\rangle \tag{13}$$

Then the energy of the system becomes

$$E = -H_{eff}\mu s_i - H_{ext}\mu s_i \tag{14}$$

Exercise 3: The magnetization in an infinite 2D lattice of dipoles

We don't want to compute the interaction every dipole has with every other dipole near it in an infinite lattice, so we will instead implement the mean field theory using the results from example 2 and generalizing them for the entire system.

If we look at a single dipole, if there is no external magnetic field, the only magnetic field it experiences is that produced by the other dipoles in the system. To make the mean field approximation, we will consider the effective field created by the nearest neighbors of a dipole and generalize it to the system as a whole.

In exercise 1 we found from (8) that

$$\langle s_i\rangle = \tanh\left(\frac{\mu H_{ext}}{kT}\right) \tag{15}$$

In this example, the lattice is not in an external magnetic field, although each dipole experiences the effective magnetic field of the dipoles surrounding it, so we will replace H_{ext} with the H_{eff} we found in (13). We will drop the subscript on$\langle s_i\rangle$ since we have a ferromagnetic system, and this dipole will align itself to have the same value as $\langle s\rangle$.

$$\langle s\rangle = \tanh\left(\frac{\mu\left(\frac{nJ}{\mu}\langle s\rangle\right)}{kT}\right) = \tanh\left(\frac{nJ\langle s\rangle}{kT}\right) \tag{16}$$

We can calculate the magnetization of the system by noting that

$$M = n\mu\langle s\rangle \tag{17}$$

Furthermore, when all of the dipoles perfectly aligned with each other, the average spin of the dipoles will be one, and the magnetization will be at saturation. Let the magnetization saturation be given by

$$M_s = n\mu \tag{18}$$

It follows that the average spin alignment is the ratio of the magnetization to saturation magnetization; then

$$\frac{M}{M_s} = \tanh\left(\frac{nJM}{kTM_s}\right) \tag{19}$$

However we can define the Curie temperature as $T_c = {}^{nJ}/_{k}$ so (19) becomes

$$\frac{M}{M_s} = \tanh\left(\frac{T_c M}{TM_s}\right) \tag{20}$$

(20) is a transcendental equation and can be solved graphically. By plugging in various temperatures, we find that there are three solutions at some temperatures, two of which are equal and opposite, since the system has no preference of how we define spin up and spin down, and a third unstable solution at M=0. The M=0 solution is unstable because the system prefers to have some dipole alignment or spontaneous magnetization. However, above a certain temperature, we find that there is only one solution at M=0. This suggests the existence of a Curie temperature, below which the system has spontaneous magnetization. Above the Curie temperature, the energy of the system becomes great enough such that dipole alignment no longer becomes energetically favorable, and all spontaneous magnetization is lost. The first temperature at which the system only has one solution is the Curie temperature, and both sides of (20) have a slope of 1 at M=0 for this solution. However, by recalling the definition of tanh, we can rearrange (20) in the following way by letting $x = e^{\frac{MT_c}{M_s T}}$

$$\frac{M}{M_s} = \tanh(x) = \frac{\left(x - \frac{1}{x}\right)}{\left(x + \frac{1}{x}\right)}$$

and rearranging algebraically to find that

$$\frac{T}{T_c} = {}^{\left(\frac{2M}{M_s}\right)}\Big/_{\ln\left(\frac{M}{M_s}+1\right) - \ln\left(\frac{M}{M_s}-1\right)} \tag{21}$$

Finally, we get (21) and can compare the reduced temperatures and magnetizations. One example of a solution curve looks like this, for a 3 dimensional tetragonal model, rather than a 2D lattice.

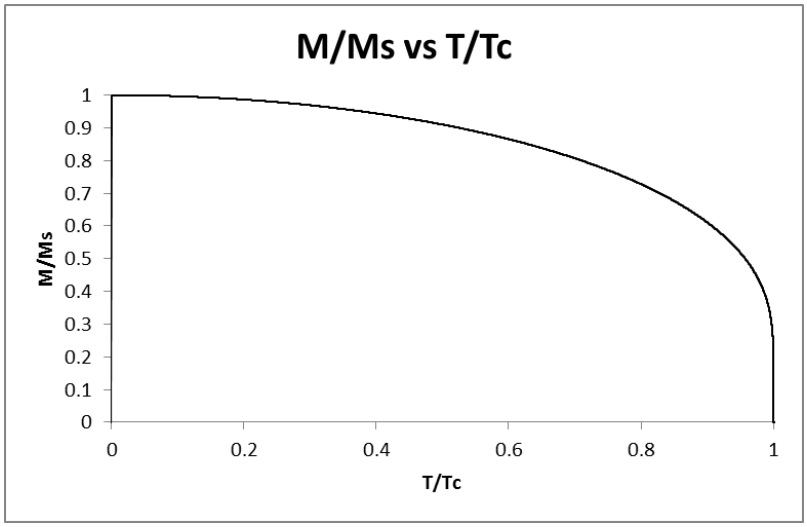

Figure 7 The normalized magnetization of the system as a function of the normalized temperature

Since we can calculate the saturation magnetization from (18), and we know the Curie temperature, we can use (21) to then make predictions for the magnetization of a system based on temperature. From there we could also make predictions for the magnetic field strength of a magnet as a function of temperature.

Appendix II- Elements of Statistical Physics

Boltzmann Statistics are useful for calculating the probability of finding a system in any particular microstate when the system behaves quasistatically at thermal equilibrium. The microstates of a system are defined by the energy levels available to it, and there typically exist many degenerate states with the same energy. For example, when considering a single magnetic dipole with no external magnetic field applied to it, the dipole has two degenerate states, spin up and spin down, that have the same energy.

To find the probabilities of finding a system in a particular state, Boltzmann factors are compared to the partition function of a system, where

$$Boltzmann\ factor = e^{-\frac{E(s)}{kT}}\ and$$

$$The\ Partition\ Function, \mathcal{Z} = \sum_{s} e^{-\frac{E(s)}{kT}}$$

$$= the\ sum\ of\ all\ Boltzmann\ Factors$$

And the probability of finding a system in one particular state is given by

$$\boldsymbol{\mathcal{P}}(\mathrm{s}) = \frac{1}{\boldsymbol{\mathcal{Z}}} e^{-\frac{E(s)}{kT}}$$

This is known as the Boltzmann distribution or canonical distribution, where E(s) is the energy of a particular state, k is Boltzmann's constant and T is the absolute temperature of the system. Finding the partition function can be difficult, especially in large systems, and often the terms drop off quickly, so only the first few are calculated. Readers are encouraged to refer to Daniel Schroeder's An Introduction to Thermal Physics, particularly sections 6.1-6.3.

Appendix III- Calculation of the Magnetic Field Strength Using Surface Bound Currents

Exercise 1: Calculating magnetic fields from a given magnetization.

Perhaps we want to find the actual magnetic field produced as a result of the magnetizations we have predicted in an actual magnet. In (26) we found the normalized values we would expect for the magnetization in a system based on the normalized temperatures of the system. To predict an actual value for the magnetization, we can multiply the normalized magnetization by the saturation magnetization, and multiply the normalized temperatures by the Curie temperature. For a real system, such as a neodymium rare earth magnet, the material forms tetragonally shaped dipoles, and each dipole has 6 neighbors. Therefore, we can use (18) to find the saturation magnetization

$$M_s = n\mu = 6\mu_B = 5.5644054 \times 10^{-23}\, J/T$$

Additionally, the Curie temperature of neodymium magnets has be well established as

$$T_C = 583.15K$$

From this we can predict what the magnetization should be in the neodymium magnet as a function of temperature. From here we can calculate the magnetic field strength knowing that

$$\boldsymbol{H} = -\boldsymbol{\nabla}\Psi \tag{27}$$

Where Ψ is the magnetic scalar potential. From the flux continuity law, we know that

$$\nabla \cdot \boldsymbol{H} = -\nabla \cdot \boldsymbol{M} \tag{28}$$

If we integrate both sides of the flux continuity law over an incremental volume, we find that

$$\int \boldsymbol{\nabla} \cdot \boldsymbol{H} = \int -\boldsymbol{\nabla} \cdot \boldsymbol{M} \;;\; \int \boldsymbol{\nabla} \cdot \mu_o \boldsymbol{H} = \int -\boldsymbol{\nabla} \cdot \mu_o \boldsymbol{M}$$

$$\boldsymbol{n} \cdot \mu_o(\boldsymbol{H^a} - \boldsymbol{H_b}) = \boldsymbol{n} \cdot \mu_o(\boldsymbol{M^a} - \boldsymbol{M_b}) \tag{29}$$

where μ_o is the permeability of free space and not to be confused with μ, the magnetic dipole moment. $\boldsymbol{H^a}$ and $\boldsymbol{H_b}$ denote the magnetic fields on the top and bottom of the object while $\boldsymbol{M^a}$ and $\boldsymbol{M_b}$ denote the magnetization on the top and bottom surfaces of the object. We use the right hand side of (28) and (29) to define ρ_m, the magnetic charge density, and σ_m, the magnetic surface charge density.

$$\rho_m \equiv -\boldsymbol{\nabla} \cdot \mu_o \boldsymbol{M}\,, \sigma_m = \boldsymbol{n} \cdot \mu_o(\boldsymbol{M^a} - \boldsymbol{M_b})$$

Where $\vec{n}$ is the normal vector of the surface being looked at and $(\boldsymbol{M^a} - \boldsymbol{M_b})$ refers to the upper and lower surfaces, respectively. We then take the divergence of (27) to find that

$$\boldsymbol{\nabla} \cdot \boldsymbol{H} = \boldsymbol{\nabla} \cdot (-\boldsymbol{\nabla}\Psi) = -\boldsymbol{\nabla}^2\Psi \tag{30}$$

Again, from the flux continuity law, it follows that Ψ must follow Poisson's equation, so

$$\boldsymbol{\nabla}^2\Psi = -\frac{\rho_m}{\mu_o} \text{ so}$$

$$\Psi = \int_{V'} \frac{\rho_m(\boldsymbol{r}')dv'}{4\pi\mu_o|\boldsymbol{r} - \boldsymbol{r}'|} + \int_{S'} \frac{\sigma_m(\boldsymbol{r}')\rho' d\rho'}{4\pi\mu_o|\boldsymbol{r} - \boldsymbol{r}'|} \tag{31}$$

Suppose we have a cylindrically shaped magnet, which has a uniform magnetization throughout it, so $\mu_o \boldsymbol{M} = \mu_o M_0$. Then the divergence of the magnetic volume charge density is zero, so the first integral of the right hand side of (29) is zero. We find that

$$\rho_m \equiv -\boldsymbol{\nabla} \cdot \mu_o \boldsymbol{M} = 0, \sigma_m = \boldsymbol{n} \cdot \mu_o(\boldsymbol{M^a} - \boldsymbol{M_b}) = \pm\mu_o M_0$$

We could from here find the solution to (31) over all space, but to make things simpler, we will orient our coordinate system such that the direction of magnetization in the material is along the z axis only, and then find the magnetic scalar potential along the z axis. (31) becomes a superposition integral as we integrate over the top and bottom surfaces of the magnet. Note that, since the sides of the cylinder are parallel to the z axis, they make no contribution to the field along the z axis.

$$\Psi_z = \int_{S'} \frac{\sigma_m(\overrightarrow{r'})\rho' d\rho'}{4\pi\mu_o|\overrightarrow{r} - \overrightarrow{r'}|}$$

$$= \int_0^R \frac{\mu_o M_0 \, 2\pi\rho' d\rho'}{4\pi\mu_o \sqrt{\rho'^2 + \left(z - \frac{d}{2}\right)^2}} + \int_0^R \frac{-\mu_o M_0 \, 2\pi\rho' d\rho'}{4\pi\mu_o \sqrt{\rho'^2 + \left(z + \frac{d}{2}\right)^2}}$$

$$= \frac{2\pi\mu_o M_0}{4\pi\mu_o} \int_0^R \frac{\rho' d\rho'}{\sqrt{\rho'^2 + \left(z - \frac{d}{2}\right)^2}} - \int_0^R \frac{\rho' d\rho'}{\sqrt{\rho'^2 + \left(z + \frac{d}{2}\right)^2}}$$

$$= \frac{M_0}{2} d \cdot \left[\sqrt{\left(\frac{R}{d}\right)^2 + \left(\frac{z}{d} - \frac{1}{2}\right)^2} - \left|\frac{z}{d} - \frac{1}{2}\right| - \sqrt{\left(\frac{R}{d}\right)^2 + \left(\frac{z}{d} + \frac{1}{2}\right)^2} + \left|\frac{z}{d} + \frac{1}{2}\right| \right]$$

We then take the gradient of this, and find $\vec{H}$ in (27)

$$\overrightarrow{H_z} = -\nabla \Psi_z$$

$$= -\nabla \left(\frac{M_0}{2} d \cdot \left[\sqrt{\left(\frac{R}{d}\right)^2 + \left(\frac{z}{d} - \frac{1}{2}\right)^2} - \left|\frac{z}{d} - \frac{1}{2}\right| - \sqrt{\left(\frac{R}{d}\right)^2 + \left(\frac{z}{d} + \frac{1}{2}\right)^2} + \left|\frac{z}{d} + \frac{1}{2}\right| \right] \right)$$

$$\overrightarrow{H_z} = -\frac{d \cdot M_0}{2} \left[\frac{\left(\frac{z}{d} - \frac{1}{2}\right)}{\sqrt{\left(\frac{R}{d}\right)^2 + \left(\frac{z}{d} - \frac{1}{2}\right)^2}} - \frac{\left(\frac{z}{d} + \frac{1}{2}\right)}{\sqrt{\left(\frac{R}{d}\right)^2 + \left(\frac{z}{d} + \frac{1}{2}\right)^2}} \right] \text{ outside of the magnet} \qquad (30)$$

We can plug in the values for M_0 that we found using (26) to predict how the magnetic field strength of a magnet should change as a function of temperature for a cylindrically shaped magnet with R= 7/8 in (1.11 cm) and d= 1/4 in (0.635 cm).

Appendix IV- Experimental Data and Analysis

A selected sample of the observed magnetic flux density is shown in Table 1 below, with the sample data plotted in figure 8.

		using 16.81687x+0.228906
Temp (K)	Voltage (V)	Bz (G)
77.153393	0.740379	12.67976339
87.154098	0.742568	12.71657552
97.776867	0.743498	12.73221521
107.555447	0.745772	12.77045677
118.862619	0.746888	12.7892244
127.87265	0.751015	12.85862762
137.468743	0.773553	13.23764624
147.951575	0.799409	13.67246323
157.881295	0.805553	13.77578608
167.889339	0.804523	13.7584647
177.872436	0.801691	13.71083933
187.804135	0.7979	13.64708657
197.310836	0.792743	13.56036197
207.903393	0.786091	13.44849616
217.999629	0.77974	13.34169221
227.897274	0.775191	13.26519227
237.861586	0.77027	13.18243645
247.960983	0.761336	13.03219454
257.970111	0.753068	12.89315266
267.982672	0.747267	12.79559799
277.979582	0.739392	12.66316514
281.918716	0.736967	12.62238423

Table 1 Sample data taken from a typical test with voltages and the calculated magnetic flux density in the second and third columns respectively. At the top right is seen the calibrated function used to convert voltages from the Hall Effect probe into Gauss.

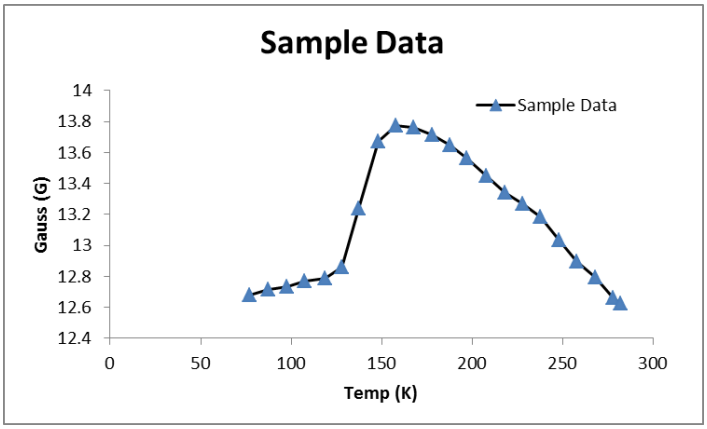

Figure 8 A plot of the magnetic flux density as a function of temperature of Table 1.

Error was propagated through the system in the form of errors in measurement of the distance of the Hall Effect probe from the magnet, the accuracies of the National Instruments 9213 and 9219 modules and the T- type thermocouple and Hall Effect probe itself. There is found to be a 4.12% error in measurement, and the sample data of table 1 is plotted in figure 9 with error bars to account for the error in measurement.

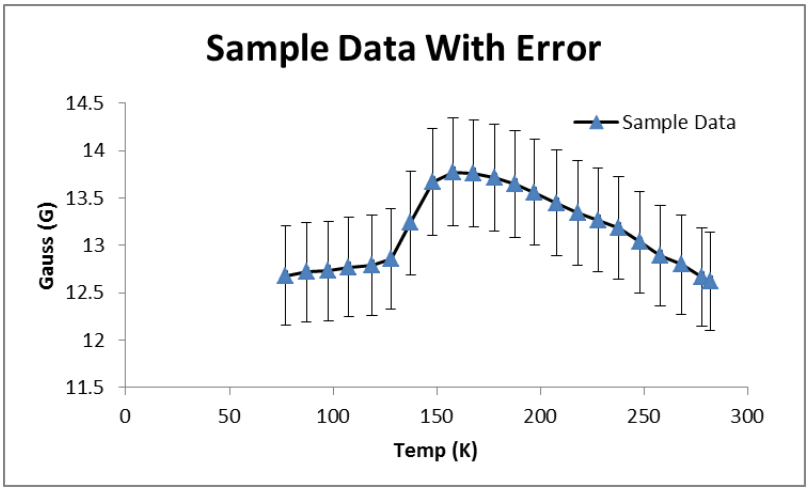

Figure 9 The sample data of table 1 with 4.12% error.

To make the mean field approximation, after the temperature dependence of the magnetization of a single dipole is calculated, this magnetization is multiplied by the total number of dipoles. To calculate the total number of dipoles, the disc shaped magnet is weighed several times to find a mass of 36.3027g. Knowing that the molecular unit weight of a single $Nd_2Fe_{14}B$ magnet is 1076.921g/mol, the number of moles in the magnet is calculated. Multiplying by Avogadro's number yields the total number of dipoles in the system. Multiplying by the magnetization of a single crystal, the magnetization in the system as a whole is calculated. The theoretical magnetization in the disc magnet calculated using this method is depicted in figure 8. The magnetizations produced from figure 10 are then used in equation (30) to calculate the magnetic field intensity at some distance away from the magnet.

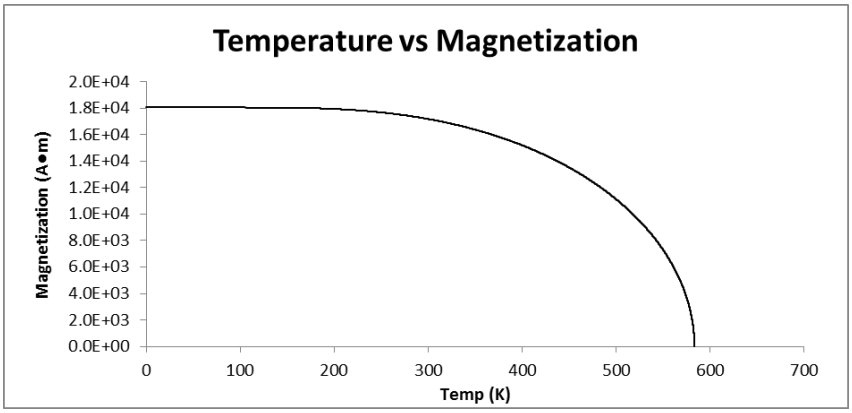

Figure 10 The calculated magnetization in the disc magnet as a function of temperature. Notice the values are quite large, but they yield reasonable results when used to calculate the magnetic field intensity.

After calculating the magnetic field intensity from the magnetizations of figure 8, the theoretical curve produced for the magnetic field intensity or magnetic flux density can be compared to the observed field.

---

[i] D. Schroeder. *An Introduction to Thermal Physics* (Pearson, New York, 2000)

[ii] N. Giordano. *Computational Physics* (Pearson, Upper Saddle Rive, NJ, 2006), 2nd ed.

[iii] M. A. B. Whitaker "Exact expressions for ferromagnetic magnetization in the mean field theory." *American Journal of Physics*, 1989: 45-47

[iv] By carefully weighing each magnet, the total number of crystals in each can be calculated by knowing the composition of each.

[v] H. Haus, J. Melcher. *Electromagnetic Fields and Energy* (Prentice-Hall, Englewood Cliffs, NJ, 1989)

[vi] E. Diez-Jimenez, *et al.,* Journal of Applied Physics **11**, 063918 (2012)